Xavier Amandolèse
Research Engineer,
Institut Aérotechnique,
15, rue Marat,
F-78210 Saint-Cyr l'Ecole, France

Pascal Hémon
Research Engineer,
Hydrodynamics Laboratory-LadHyX,
Ecole Polytechnique-CNRS,
F-91128 Palaiseau, France

Clotilde Regardin
Research Engineer,
Institut Aérotechnique,
15, rue Marat,
F-78210 Saint-Cyr l'Ecole, France

An Experimental Study of the Acoustic Oscillations by Flows Over Cavities

We present an experimental study of acoustic oscillations induced by an internal airflow over a shallow and a deep cavity. The Kelvin-Helmholtz instability is interacting with an acoustic mode of the cavity or of the duct, leading to a resonance which produces a very high sound level. The influence of upstream boundary layer thickness and neck thickness is studied. Some results obtained by modifying the upstream lip shape, by crenel addition, are also given. [DOI: 10.1115/1.1688761]

1 Introduction

The problem deals with the internal flows encountered in many industrial processes where a fluid has to be transported in a piping system. All the valves or other elements may create a flush mounted cavity as presented in Fig. 1. The shear layer usually exhibits a periodic vortex organization that can interact with some eigenmodes of the system, particularly the volume of the cavity, creating a so-called Helmholtz resonator, or an acoustic mode of the duct. This paper deals mainly with the interactions of the duct with a deep and a shallow cavity. The Helmholtz resonator [1] is similar to the phenomenon occurring in car vehicles with an opened sunroof [2].

The problem of shear layer instability has been widely studied in various situations [3]. Particularly, the impinging shear layers are known to be responsible for coherent oscillations when the wave length associated to the vortices is close to the neck length L (see Fig. 1) [4,5].

However, in order to be self-sustained, the shear layer oscillation has to interact with another system within a resonance effect. Flush-mounted cavities have been also well studied in the past [6–9]. The case of rectangular cavities, and their tone frequencies has been reviewed and studied in [10]. Recently, the resonance in piping systems has been investigated in [11].

However, the resonance problem between an impinging shear layer and an acoustic mode of a pipe is not well documented. Moreover, the influence for instance of the incoming boundary layer thickness has only been reported [12] in a non resonant configuration and requires more experiments and analysis.

The paper is organized as follows: first a deep cavity is studied, for which the resonance occurs not only with the duct but also with its volume. A shallow cavity, more common in piping systems, is then studied with various variable parameters, especially the incoming boundary layer thickness and the neck thickness, a solution for sound attenuation is proposed, based on crenels.

2 Experimental Setup

The cavities have been mounted in a small acoustic wind tunnel of the Institut Aérotechnique which generates a very low noise airflow. Details on the facility and the measurement system are available in [13]. An original feature is that it allows to measure the outside acoustic pressure P_e for a given range of frequencies even when the wind is blowing: this kind of measurement is performed by plane waves intensimetry with 3 microphones, leading to a frequency range between 80 and 660 Hz.

The acquisition system is the PAK system provided by Müller-BBM for which measurement hardware is based on the VXI standard. The acquisition card is a 16 bits A/D converter equipped with direct signal processors for Fast Fourier Transform measurements. The frequency resolution was chosen to be 0.18 Hz for the deep cavity and 0.5 Hz for the shallow one. The acoustic pressure accuracy is typically of 1 dB. The reference freestream velocity U_o is measured with an accuracy of around 1%. The temperature was also measured for each test in order to calculate the associated speed of the sound. For both the deep and shallow cavity experiments it was close to 20°C. The speed of the sound based on temperature measurement was validated by the direct estimation of c_o with plane wave intensimetry.

The pressure measurements are complimented by velocity measurements using hot wire anemometry. Boundary layer probes (Type P15 provided by Dantec) were used. The constant temperature anemometer was calibrated using a nonlinear fitting curve and the resulting accuracy is of 5%. Acquisition and numerical processing were made using the PAK system. The probes are mounted on a small vertical displacement traverse which has a position resolution of 0.1 mm.

3 The Deep Cavity

3.1 Description of the Model and Incoming Flow. The model of the cavity has been flush-mounted in a rectangular closed test section 260 mm high and 300 mm wide. Dimensions of the model are $H_g = 5$ mm, $L = 20$ mm and $V = 0.0039$ m^3. The neck section A_c is 0.004 m^2 and the spanwise dimension is 200 mm. The cavity is very deep, its height being $H_v = 10$ L. All these dimensions have been chosen in order to obtain a resonance frequency inside the intensimetry measurement range of the setup, between 80 and 660 Hz for a wind velocity around 10 to 25 m/s.

The pressure P_v in the cavity is measured by a microphone. The resonance frequency of this deep cavity was measured without wind by using an acoustic source providing a white noise in the test section. The response of the cavity gave a natural frequency of 263 Hz (± 0.5) which is in relatively good agreement with the expected value using the classical theory of the Helmholtz resonator for noncircular holes [1].

The first acoustic modes of the test section, which is rectangular, are listed in Table 1 and given by the formula

$$f_t = c_o/2a \tag{1}$$

Contributed by the Technical Committee on Vibration and Sound for publication in the JOURNAL OF VIBRATION AND ACOUSTICS. Manuscript received July 2002; Revised November 2003. Associate Editor: Keltie.

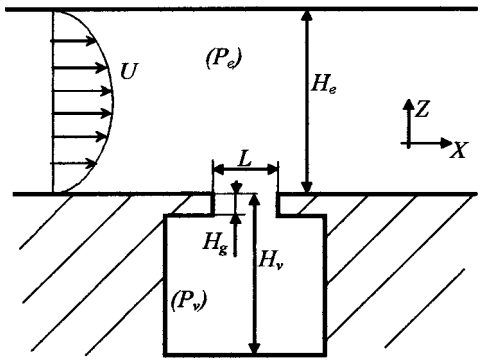

Fig. 1 Configuration of the study

where a is the length of the relevant dimension, vertical or lateral. We can see that a priori the cavity resonance is far from these values and should not interact with the test section. Furthermore, according to experiments, we found a little difference with formula (1) which is probably due to the finite length of the test section. Indeed it creates non ideal boundary conditions as it is assumed for the theoretical values.

The incoming boundary layer profile was measured in detail and given in Fig. 2 in dimensionless variables. The mean velocity and its root-mean-square (RMS) are given reduced by the mean flow rate velocity. The mean velocity profile outside the viscous sub-layer can be well fitted by a logarithmic profile, which is a typical characteristic of a fully developed, equilibrium, turbulent boundary layer, with zero pressure gradient. The resulting integral thicknesses are $\delta_1 = 4.5$ mm (displacement thickness) and $\delta_2 = 3.6$ mm (momentum thickness). It is known that the parameter δ_1/L is very important for the shear layer instability in the neck: its value here is 0.22 which is small enough to a priori allow an excitation by the first mode of the attached shear layer [12].

3.2 Frequency and Pressure Level Results. Figure 3 presents the measured acoustic pressure level P_v inside the cavity, and its corresponding frequency, versus the freestream velocity.

Table 1 Frequencies of the first acoustic modes of the test sections

Direction	Vertical	Lateral
Deep cavity	660 Hz	572 Hz
Shallow cavity	1252 Hz	1072 Hz

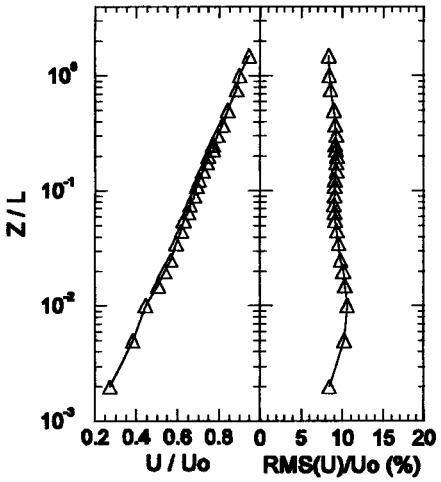

Fig. 2 Boundary layer profile at $X = -2$ L, deep cavity

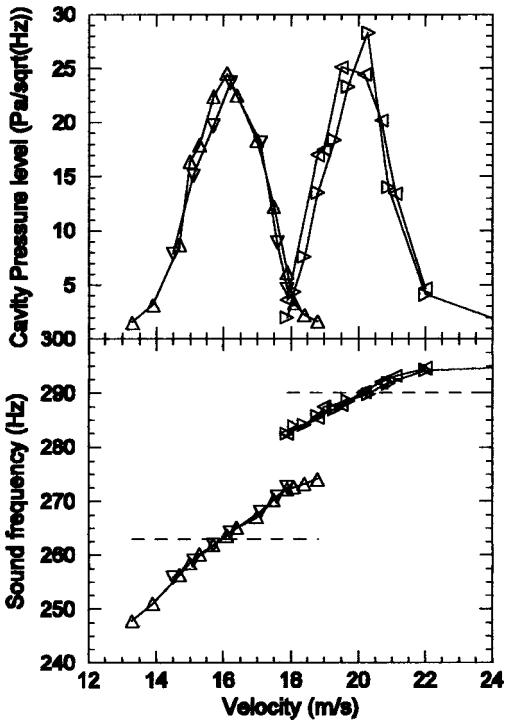

Fig. 3 Cavity pressure level and corresponding frequency versus U_o, deep cavity

(The two sets of symbol correspond to the same test made twice.) The physical unit for the pressure level is from a power spectral density and does not depend on the acquisition parameters. For a better approach of the physics, note that a pressure level of 25 $Pa/\sqrt{\text{Hz}}$ is equivalent to 115 dB with our frequency resolution, which is a very high level for the human ear.

The horizontal dashed lines on the frequency curve are the frequencies which correspond to the natural frequency of the cavity, for the first one, and to one acoustic mode frequency of the test section for the second one. Two acoustic resonance leading to very high pressure level in the cavity can be observed by increasing the velocity from 13 m/s to 22 m/s. The first one, for which the maximum pressure level is observed closed to 16 m/s is mainly due to a coupling between the shear layer excitation and the volume of the cavity. Up to 18 m/s there is an emergence of a second tone in the spectrum which creates at 290 Hz a very high pressure level for a velocity close to 20 m/s. This second resonance is induced by the first harmonic of this frequency which is locked with the lateral acoustic mode of the test section. In order to verify that the lateral dimension of the test section is really the cause of this pressure peak, this dimension was modified by adding a layer of wood on the lateral wall. Then, according to formula (1), the frequency was increased so that the resonance could not occur due to the limited range of the wind velocity. This was experimentally verified.

3.3 Transfer Function. In order to better understand the phenomenon, we measure using intensimetry the external pressure P_e, around the two resonance velocities. This is performed simultaneously with measurements of the internal pressure P_v. Then we plot the transfer function P_v/P_e in amplitude (modulus) and phase angle ϕ in Fig. 4. The main point of these data is the phase angle which is found to be 97° (±2°) at the resonance with the cavity for $U_o = 16$ m/s. At the second point of resonance ($U_o = 20$ m/s), the phase angle is very different (135°) and these differences should be physically interpreted.

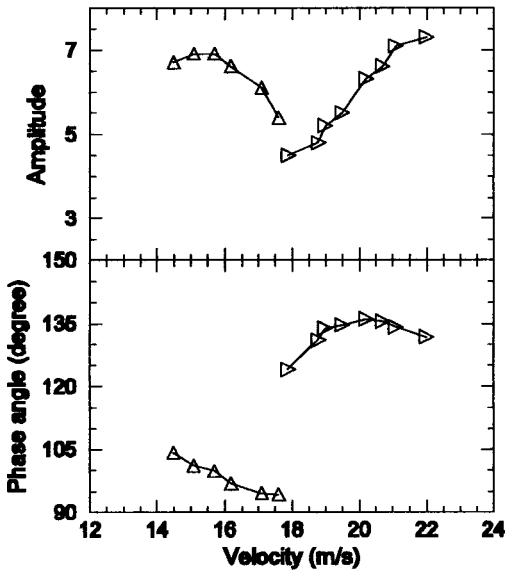

Fig. 4 Transfer function P_v/P_e versus U_o, deep cavity

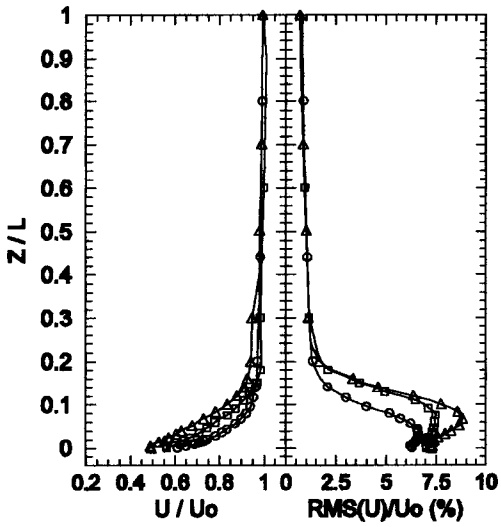

Fig. 5 Boundary layer profiles for the shallow cavity. ○: Smooth, □: Roughness 1, △: Roughness 2.

From the classical theory of the Helmholtz resonator, assuming that the air is a perfect gas and the cavity is adiabatic, we may write

$$\frac{VH_g}{c_o^2 A_c}\ddot{P}_v + P_v = P_e + \varepsilon P_{sl} \tag{2}$$

The coefficient ε is a dimensionless unknown amplitude of the excitation term P_{sl} produced in the neck by the shear layer instability. The external pressure P_e appears as an additional term depending on the confinement. Since the response is harmonic at resonance points, it can be approximately represented by means of a linear model depending upon P_v and its first derivative $\dot{P}_v$.

$$P_e = -\alpha P_v - \beta \dot{P}_v \tag{3}$$

With making the substitution of Eqs. (3) into (2) we obtain:

$$\frac{VH_g}{c_o^2 A_c}\ddot{P}_v + \beta \dot{P}_v + (1+\alpha)P_v = \varepsilon P_{sl} \tag{4}$$

For which α and β can be easily determined by means of the modulus and phase of the transfer function P_v/P_e. Indeed at resonance point the following equation can be written:

$$P_e = \left[\left|\frac{P_e}{P_v}\right|\cos(\phi) - i\left|\frac{P_e}{P_v}\right|\sin(\phi)\right]P_v \tag{5}$$

By examining the real and imaginary parts of Eqs. (3) and (5) we obtain:

$$\alpha = -|P_e/P_v|\cos(\phi) \tag{6}$$

$$\beta = \frac{1}{2\pi f}|P_e/P_v|\sin(\phi) \tag{7}$$

According to the values reported in Table 2, the system is not only a simple resonator excited by a shear layer tuned in frequency. Indeed, the confinement of the flow above the cavity produces a damping term and a stiffness term, with associated coefficients, β and α, which are both positives.

It can be noticed in Table 2, that the damping is much smaller for the second peak: this is physically logical, the confinement being itself the cause of this resonance. Moreover, the coefficient of added stiffness α is much larger for the resonance involving the test section, which is again logical from a physical point of view. It explains also why the frequency of the second peak is higher than the natural cavity resonance, since the total stiffness is increased by 10.7%. This leads to a square root increase in frequency, which agrees with the measured frequency of the second peak (within an uncertainty range).

Table 2 Measured parameters of the system

	First peak At $f_v = 263$ Hz	Second peak At $f = 290$ Hz
P_v/P_e	6.6	6.6
ϕ	97°	135°
α	0.0185	0.107
β	$9.1\ 10^{-5}$	$5.9\ 10^{-5}$

4 The Shallow Cavity

4.1 Description of the Model and Incoming Flow. The shallow cavity is mounted in the same way as the deep one, behind a test section 160 mm wide and 137 mm high. The purpose of this smaller section is to be able to increase the velocity according to the capabilities of the setup in terms of flow rate. Expected Mach numbers are in the range [0.10–0.25].

The cavity dimensions in mm are $L = 50$, $H_v = 20$, and 150 spanwise. The neck thickness H_g is variable, between 2 and 8 mm. The neck section is $A_c = 0.0075\ \text{m}^2$ and the volume is $V = 0.00013\ \text{m}^3$. It is not expected here to obtain an excitation of the cavity volume by the shear layer, as in a Helmholtz resonator. However, a resonance between the shear layer frequency and the vertical acoustic mode of the test section, given in Table 1, is expected.

Nevertheless, it was shown in [12] that the incoming boundary layer thickness was an important parameter of such a problem, even if this study is not completely transposable to ours. These experiments showed that a small boundary layer thickness (usually reduced by the neck length) is able to induce the shear layer oscillations on the first mode ($n = 1$ in Rossiter's formula), although a larger thickness is exciting the higher orders. Anyhow in the present study, the model of the cavity and its associated test section are designed in order to reach a frequency range of resonance corresponding to the second order mode of Rossiter ($n = 2$).

The measured boundary layer profiles 5 mm upstream the shallow cavity are given in Fig. 5. The vertical origin is the wall of the tunnel. The smooth wall case leads to a boundary layer at equi-

Table 3 Integral thicknesses of the boundary layers for the shallow cavity

	$\delta 1$ (mm)	$\delta 2$ (mm)	$\delta 1/L$
Smooth wall	1.42	1.26	0.0284
Roughness 1	1.65	1.26	0.0330
Roughness 2	2.94	2.25	0.0588

librium. Some roughnesses, consisting in glued sand paper sheets, are used in order to increase the thickness. These two cases create thicker boundary layers which are not at equilibrium, as can be seen on the shape of the mean velocity profiles. The integral thickness for the three cases are given in Table 3. The second roughness leads to a thickness twice as the smooth wall.

4.2 Cavity Pressure Evolution. Figure 6 presents the acoustic pressure level inside the cavity and the corresponding frequency for the main observed peak, versus the Mach number, i.e. the velocity. The dashed line with the frequency curves correspond to the acoustic vertical mode. The two extreme cases of neck thickness are shown, the smallest one leading to a very high pressure level. This result will be discussed in section 4.3.

The dimensionless frequencies corresponding to those of Fig. 6 are plotted in Fig. 7. In this figure, we have also added (dot-dashed line) an illustrative prediction of the tone frequency based on Rossiter's formula.

The dimensionless frequencies of the oscillations of a shear layer are well approximated by Rossiter's formula [14]

$$St = n - \gamma/(M + U_o/U_c), \tag{8}$$

where n is the order of the mode and γ the empirical parameter linked to the shape of the lips and usually equal to 0.25 for sharp edges and rectangular cavities (see [10] for a review). The ratio of the convection velocity U_c to the freestream velocity U_o is almost universal and equal to 0.57.

Although Rossiter developed his tone frequency formula for a cavity whose geometry is different from that used here, the frequency measurements are relatively in good agreement with Rossiter's formula for lower velocities before the lock-in. Meanwhile measurements give larger Strouhal numbers which are in agreement with [10] for the low Mach number range of the study. For Mach numbers up to 0.18 the lock-in of the shear layer oscillation with the acoustic mode of the test section is clearly visible and the cavity frequency evolution can no more be predicted by an impinging shear layer instability type prediction such as Rossiter's formula.

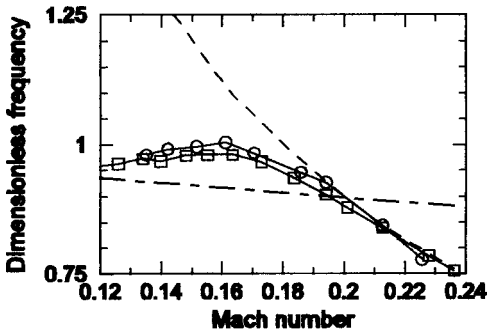

Fig. 7 Dimensionless frequencies versus M, shallow cavity. □: H_g=2 mm, ○: H_g=8 mm.

At lock-in, the velocity profiles in the shear layer are given in Figs. 8 and 9 for the longitudinal positions 0.5 L and 0.88 L respectively. The profile of the velocity Power Spectral Density (PSD) at the resonance frequency is also given. The velocity oscillations are very large even at a relatively high level above the neck, and its spatial amplitude is growing along the longitudinal axis.

4.3 Influence of the Boundary Layer Thickness. The influence of the boundary layer thickness is reported in Fig. 10 where we have plotted the main peak (pressure level and corresponding frequency) versus the displacement thickness. The thicker boundary layers lead to a large decrease of the sound level.

However, from a physical point of view, this parameter should be associated to the total thickness of the shear layer which is located at the upstream lip of the cavity: the neck thickness H_g is an important part of it. Its influence is shown in Fig. 11 for the minimum value of 2 mm up to 8 mm which is the standard configuration. Nevertheless, the effective total thickness of the shear layer is closer to an equivalent H_g given by $H_{geq} = H_g + \delta_1$: all the previous results are then collected together in Fig. 12. The isolated star symbol corresponds to a test with H_g=2 mm and

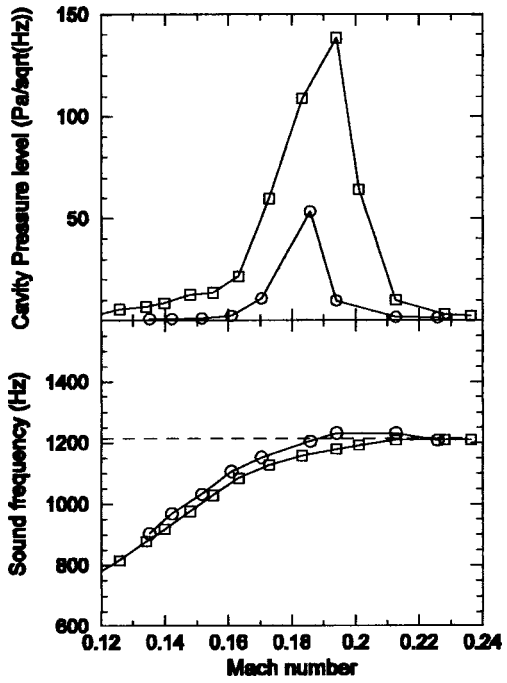

Fig. 6 Cavity pressure level and corresponding frequency versus M, shallow cavity. □: H_g=2 mm, ○: H_g=8 mm.

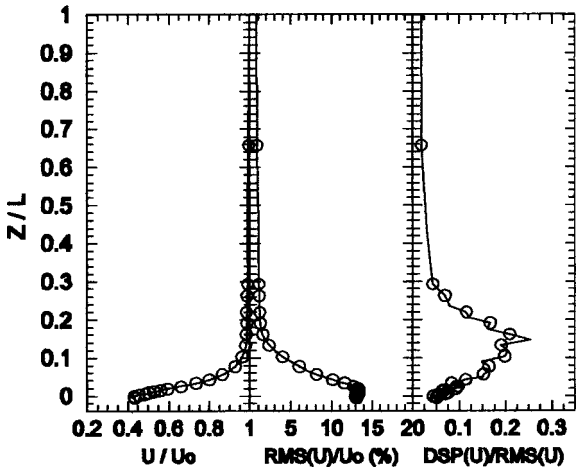

Fig. 8 Shear layer velocity profiles, shallow cavity, H_g =8 mm, M=0.187, midlength of the neck

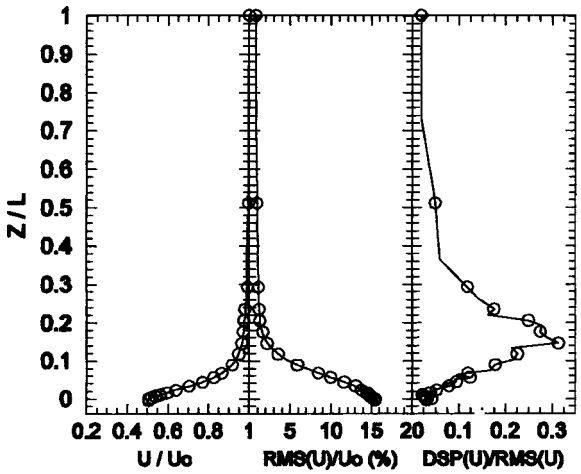

Fig. 9 Shear layer velocity profiles, shallow cavity, H_g = 8 mm, M = 0.187, 0.88 L from upstream lip

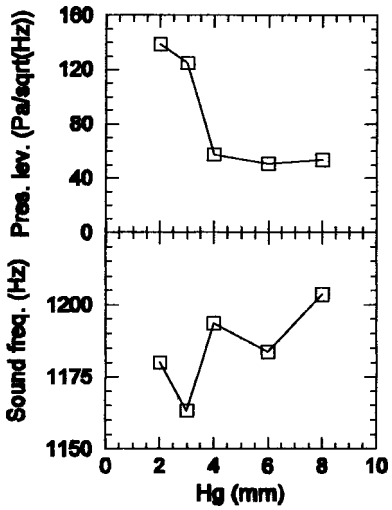

Fig. 11 Maximum pressure levels and corresponding frequencies versus H_g, shallow cavity, small boundary layer thickness

roughness 1. There is a critical value around H_{geq} = 9.5 mm which leads to a strong decrease, close to cancellation, of the resonance peak. This critical value was also detected in [12] where it was noticed that no cavity oscillation occurs when L/H_{geq} is below 5.25 (one has L = 50 mm here), even for a cavity configuration which differs from ours.

A second critical value is around H_{geq} = 5 mm (L/H_{geq} = 10) below (resp. above) which the sound level is significantly increased, whereas it is almost constant for H_{geq} between 5 to 9.5 mm. Although it is less obvious with the additional test (star symbol), its level is however also increased. This second critical value requires further investigations to better understand the reason of this jump.

It may also be noticed that there exists an increase of the frequency oscillation with this parameter, the slope of which (using a linear least square approximation) is 5 Hz/mm. This leads to an increase of the Strouhal number according to formula:

$$St = 0.20 H_{geq}/L + St_o, \tag{9}$$

where St_o = 0.93 corresponds to the dimensionless frequency obtained for a zero thickness.

4.4 Sound Attenuation. We have seen above that the increase of the boundary layer thickness is a very good means to attenuate the sound. In a piping system a great disadvantage of this is the increase of the pressure loss. Addition of a deflector just upstream would have the same effect. Other solutions have therefore been explored: the problem is that the allowed modifications are generally limited by the kinematics of the valve for example.

Since the shear layer oscillation is due to a series of vortex rolls which are quasi two-dimensional at resonance, a spanwise decrease of the vortex correlation should reduce the resonant excitation. Figure 13 presents a design of crenels made on the upstream lip. Their width is 5 mm, with a distance of 20 mm between their axis; the resulting configuration is called ''crenels 1/4'' (5 mm over 20 mm). Another configuration has been implemented, called ''crenels 1/2'' which has 10 mm wide crenels. The third tested solution was the ''right crenels 1/4'' which has the same size as the ''crenels 1/4'' but with a sectional shape forming a backward facing step instead of a 45° bevel edge.

The results of the tests are given in Table 4 where only the maximum pressure level is given. The ''crenels 1/4'' configuration has almost the same efficiency as the ''crenels 1/2.'' It is interesting to see that the shape of the crenels is important, since the ''right crenels 1/4'' produces a significant attenuation, the pressure being divided by a factor larger than 3.

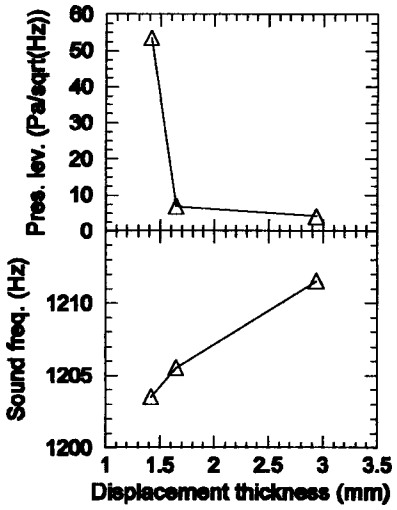

Fig. 10 Maximum pressure levels and corresponding frequencies versus $\delta 1$, shallow cavity, H_g = 8 mm

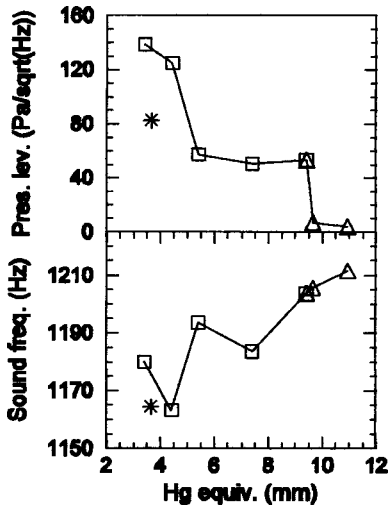

Fig. 12 Maximum pressure levels and corresponding frequencies versus $H_g + \delta 1$ for the shallow cavity

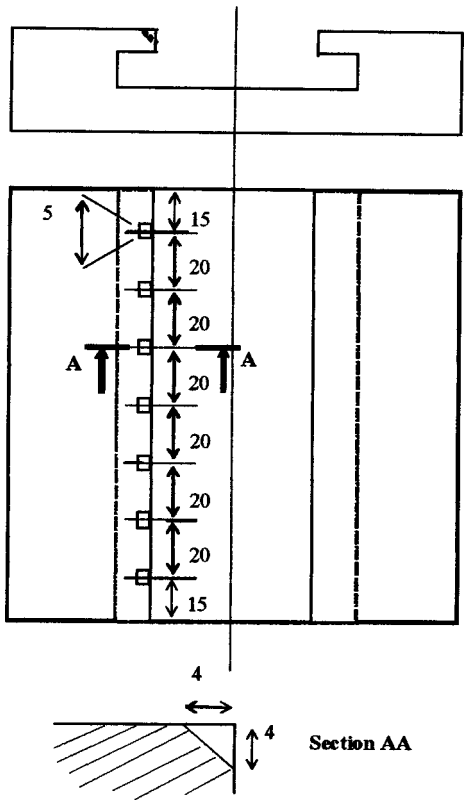

Fig. 13 Upstream lip modification for sound attenuation, "crenels 1/4"

Table 4 Maximum pressure levels with sound attenuation systems, shallow cavity, H_g=8 mm, small boundary layer

Configuration	Pressure level (Pa/$\sqrt{}$Hz)
Standard	53.3
Crenels 1/4	23.0
Crenels 1/2	23.5
Right crenels 1/4	15.9

Conclusion

Experiments have been presented concerning the interaction of the shear layer created by confined flows over cavities with a pipe acoustic mode. The application lies in the sound generated in piping systems due to singularities such as valves.

The cases of a deep and a shallow cavity have been tested, the first one being close to a so-called Helmholtz resonator. It was shown by measurements that the added damping due to the confinement is smaller when the resonance occurs with the duct, than when the resonance occurs classically with the Helmholtz resonator.

The shallow cavity was studied parametrically according to the boundary layer and neck thicknesses. Critical values have been detected but further investigations have to be performed and analyzed. A few passive sound attenuation techniques have also been explored, by modifying the upstream lip shape. The crenels consisting in a backward facing step were found the most efficient.

Acknowledgments

The study of the shallow cavity was performed at the Institut Aérotechnique in association with the department of Analysis in Mechanics and Acoustic of Electricité de France, within the research contract No E27312.

Nomenclature

A_c = section area of the neck
c_o = sound velocity
δ = boundary layer thickness
δ_1 = displacement thickness
δ_2 = momentum thickness
f_r = reduced frequency ($=fL/U_o$)
f_{sl} = frequency in the shear layer
f_t = mode frequency of the test section
f_v = cavity natural frequency
f = sound frequency
H_g = cavity neck depth
H_v = cavity total depth
L = cavity neck width
M = Mach number ($=U_o/c_o$)
P_{sl} = acoustic pressure in the shear layer
P_e = acoustic pressure outside cavity
P_v = acoustic pressure inside cavity
St = Strouhal number ($=f_{sl}L/U_o$)
U_o = freestream velocity
V = volume of the cavity

References

[1] Crighton, D. G., Dowling, A. P., Ffowcs Williams, J. E., Heckl, M., and Leppington, F. G., 1994, *Modern Methods in Analytical Acoustics*, Springer-Verlag, London.
[2] Kook, H., Mongeau, L., Brown, D. V., and Zorea, S. I., 1997, "Analysis of the Interior Pressure Oscillations Induced by Flow Over Vehicle Openings," Noise Control Eng. J., **45**(6), pp. 223–234.
[3] Ho, C.-M., and Huerre, P., 1984, "Perturbed Free Shear Layers," Annu. Rev. Fluid Mech., **16**, pp. 365–425.
[4] Ziada, S., and Rockwell, D., 1982, "Oscillations of an Unstable Mixing Layer Impinging Upon an Edge," J. Fluid Mech., **124**, pp. 307–334.
[5] Rockwell, D., 1983, "Oscillations of Impinging Shear Layers," AIAA J., **21**(5), pp. 645–664.
[6] Naudascher, E., and Rockwell, D., 1994, Flow-induced Vibrations, Balkema, Rotterdam.
[7] Luca, M. J., et al., 1995, "The Acoustic Characteristics of Turbomachinery Cavities," NASA CR 4671.
[8] Massenzio, M., 1977, "Caractérisation des sources aéroacoustiques sur trains grande vitesse en vue de la prévision de la pression acoustique interne," Thesis of INSA Lyon, France.
[9] Noger, C., 1999, "Contribution à l'étude des phénomènes aéroacoustiques se développant dans la baignoire et autour des pantographes du TGV," Thesis of Université de Poitiers, France.
[10] Tam, C. K. W., and Block, P. J. W., 1978, "On the Tones and Pressure Oscillations Induced by Flow Over Rectangular Cavities," J. Fluid Mech., **89**, pp. 373–399.
[11] Ziada, S., and Shine, S., 1999, "Strouhal Numbers of Flow-excited Acoustic Resonance of Closed Side Branches," J. Fluids Struct., **13**, pp. 127–142.
[12] Sarohia, V., 1977, "Experimental Investigation of Oscillations in Flows Over Shallow Cavities," AIAA J., **15**(7), pp. 984–991.
[13] Hemon, P., 2000, "Mesure des caractéristiques acoustiques de singularités aérauliques en présence de l'écoulement," *SIA Colloquium on Confort automobile et ferroviaire*, Le Mans, 15 & 16 novembre, SIA paper No CAF/00-28.
[14] Rossiter, J. E., 1964, "Wind Tunnel Experiments on the Flow Over Rectangular Cavities at Subsonic and Transonic Speed," Aero. Res. Counc. R. & M., No. 3438.